Novel CineECG Derived from Standard 12-Lead ECG Enables Right Ventricle Outflow Tract Localization of Electrical Substrate in Patients with Brugada Syndrome

Running title: *van Dam & Locati et al.; CineECG shows RVOT localization of Brugada Pattern*

Peter M. van Dam, PhD[1,3]*; Emanuela T. Locati, MD, PhD[2]*; Giuseppe Ciconte, MD[2]; Valeria Borrelli, PhD[2]; Francesca Heilbron, MD[5]; Vincenzo Santinelli, MD[2]; Gabriele Vicedomini, MD[2]; Michelle M. Monasky, PhD[2]; Emanuele Micaglio, MD[2]; Luigi Giannelli, MD[2]; Valerio Mecarocci, MD[2]; Žarko Ćalović, MD[2]; Luigi Anastasia, PhD[2,4]; Carlo Pappone, MD, PhD[2]

[1]Department of Cardiology, University Medical Center Utrecht, The Netherlands; [2]Department of Arrhythmology and Electrophysiology, IRCCS Policlinico San Donato, San Donato Milanese, Milan, Italy; [3]ECG Excellence BV, Nieuwerbrug aan den Rijn, The Netherlands; [4]Vita-Salute San Raffaele University; [5]Milano Bicocca University, Istituto Auxologico Italiano San Luca, Milan, Italy
*contributed equally

Correspondence:

Emanuela T. Locati, MD, PhD

Department of Arrhythmology and Electrophysiology

IRCCS Policlinico San Donato

Piazza E. Malan 2

20097 San Donato Milanese, Milano, Italy

Phone/Fax: +390252774260/4306

E-mail: emanuelateresina.locati@grupposandonato.it

Journals Subject Terms: Arrhythmias; Electrophysiology; Sudden Cardiac Death; Ventricular Fibrillation; Electrocardiology (ECG)

1

Abstract:

Background - In Brugada Syndrome (BrS), diagnosed in presence of a spontaneous or Ajmaline-induced type-1 pattern, ventricular arrhythmias originate from the right ventricle outflow tract (RVOT). We developed a novel *Cine*ECG method, obtained by inverse electrocardiogram (*iECG*) from standard 12-lead ECG, to localize the electrical activity pathway in BrS patients.

Methods - The CineECG enabled the temporo-spatial localization of the ECG waveforms, deriving the mean temporo-spatial isochrone (*m*TSI) from standard 12-lead ECG. The study sample included: a) 15 spontaneous BrS patients, and b) 18 Ajmaline-induced BrS patients (at baseline and after Ajmaline), in whom epicardial potential duration maps (PDM) were available; c) 17 type-3 BrS pattern patients not showing type-1 BrS pattern after Ajmaline (Ajmaline-negative); d) 47 normal subjects; e) 18 right bundle branch block (RBBB) patients. According to *CineECG* algorithm, each ECG was classified as *"Normal", "Brugada", "RBBB", or "Undetermined"*.

Results - In spontaneous or Ajmaline-induced BrS patients, *Cine*ECG localized the terminal mTSI forces in the RVOT, congruent with the arrhythmogenic substrate location detected by epicardial PDMs. The RVOT location was never observed in normal, RBBB, or Ajmaline-negative patients. In most Ajmaline-induced BrS patients (78%), the RVOT location was already evident at baseline. The *CineECG* classified all normal subjects and Ajmaline-negative patients at baseline as *"Normal"* or *"Undetermined"*, all RBBB patients as "RBBB", while all spontaneous and Ajmaline-induced BrS patients as *"Brugada"*. Compared to standard 12-lead ECG, CineECG at baseline had a 100% positive predictive value and 81% negative predictive value in predicting Ajmaline-test results.

Conclusions - In spontaneous and Ajmaline-induced BrS patients, the *Cine*ECG localized the late QRS activity in the RVOT, a phenomenon never observed in normal, RBBB, or Ajmaline-negative patients. The possibility to identify the RVOT as the location of the arrhythmogenic substrate by the non-invasive *Cine*ECG, based on the standard 12-lead ECG, opens new prospective for diagnosing BrS patients.

Nonstandard Abbreviations and Acronyms

BrS = Brugada syndrome

*Cine*ECG = Moving trajectory of the cardiac electrical activity

ECG = Electrocardiogram

*i*ECG = Inverse electrocardiogram

RBBB = Right bundle branch block

LV = Left ventricle

PDM = Potential duration maps

RV = Right ventricle

RVOT = Right ventricular outflow tract

*m*TSI = mean Temporal spatial isochrones

TCR = Trans cardiac ratio

VCG = Vectorcardiogram

VA = Ventricular arrhythmias (VA)

Introduction

Brugada syndrome (BrS) is an inherited disorder associated with a high risk of sudden unexpected death (SUD) due to ventricular arrhythmias (VA) in young and otherwise healthy patients with apparently normal hearts [1-3]. The diagnosis of BrS is achieved in the presence of either a spontaneous or drug-induced type-1 Brugada pattern in the 12-lead electrocardiogram (ECG) [1-3], characterized by a typical coved elevation of the ST interval specifically observed in

V1-V2 precordial leads [4]. The *SCN5A* gene is currently the most frequently involved, accounting for about 30% of BrS cases [4], but several other genes have also been advocated [5].

In BrS patients, the cardiac electrophysiological substrate was specifically localized at the epicardial level of the outflow tract of the right ventricle (RVOT) [6, 7]. So far, this localization could only be demonstrated by complex mapping methods, either by body surface mapping requiring the acquisition of 250 electrodes [6], or by invasive epicardial isopotential mapping [7, 8].

In spontaneous or Ajmaline-induced BrS patients, epicardial electro-anatomical voltage maps can detect the arrhythmic substrate, characterized by low-voltage (<1.5 mV) areas, generally located on the upper part of the anterior wall of the RV, which represents the area where malignant VA are originated [7, 8]. The substrate area is variable in different BrS patients before and after provocative test with Ajmaline, and the extent of the substrate area is correlated with the risk of VA[8]. The substrate area can be ablated by epicardial radiofrequency (RF) application, after which the inducibility of VA is dramatically reduced, the typical type-1 Brugada pattern is abolished, and VA can no longer be induced by Ajmaline infusion [8].

Our previous findings showed that in BrS patients, the epicardial substrate area was highly correlated with the finding of signal averaged late potentials (SAECG-LPs), which could be viewed as an expression of abnormal epicardial electrical activity [9]. Furthermore, while for many years BrS was considered a purely electric disease, our recent findings showed that the typical BrS pattern reflects an extensive RV arrhythmic substrate, even associated with consistent RV mechanical abnormalities, and that substrate ablation abolished both the Brugada pattern and mechanical abnormalities [10].

In many clinical conditions, the QRS duration taken from 12-lead ECG is a relevant discriminator between normal and pathological activation sequences. However, while the QRS

4
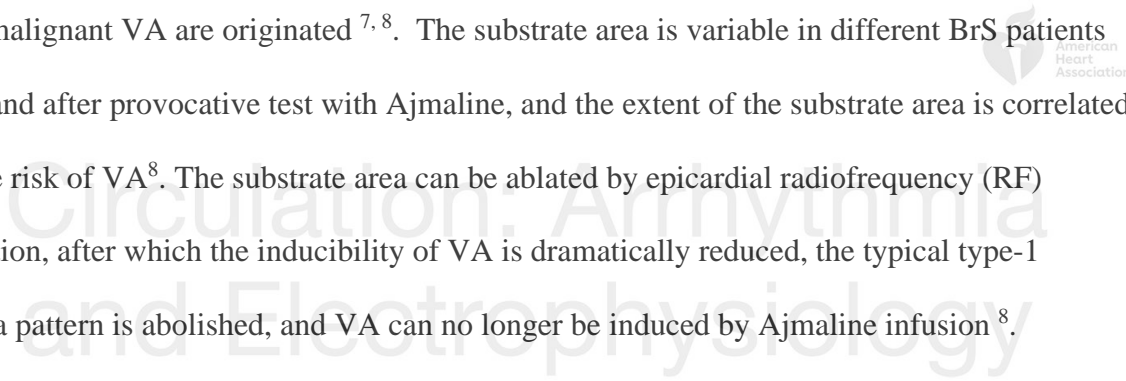
onset is generally easily detected, the QRS offset is often blurry and therefore difficult to ascertain, particularly in patients with right bundle branch block (RBBB) or in BrS patients. However, the study of these late QRS components is crucial for the detection and discrimination of such conditions. Furthermore, the 12-lead ECG interpretation is indeed a complex pattern recognition, which does not directly associate waveforms with specific cardiac structures.

Therefore, we developed a new method to measure and localize the direction of the electrical activity occurring during QRS including the early phase of the ST segment. This novel cine ECG method utilizes the inverse ECG approach (*iECG*) [11, 12], and combines ECG data with the cardiac anatomy, with the aim to overcome and facilitate the interpretation of the waveforms of the standard 12-lead ECG.

The diagnosis of BrS is often based on the Ajmaline (or Flecainide) provocative test in patients who show suspicious type 2 or 3 BrS patterns on baseline ECG, but because of the potential induction of ventricular arrhythmias, those tests should be performed under continuous medical surveillance with advanced life-support facilities. Therefore, the development of a method that might improve the interpretation and the diagnostic value of the standard 12-lead ECG is quite needed.

The aim of this study is to utilize the novel *Cine*ECG to localize the electrical activity pathway to specific cardiac areas in spontaneous or Ajmaline-induced BrS patients, in comparison with normal controls, with RBBB patients, and with patients with type 3 Brugada pattern who did not develop the type-1 Brugada Pattern after Ajmaline infusion (defined as Ajmaline negative patients).

5

Methods

Study Sample

The study sample included in this study was derived from the about 2,500 patients referred for suspected Brugada Syndrome to the Arrhythmology and Electrophysiology Unit, San Donato Hospital, Milan, Italy, in the last 5 years. Complete medical history, physical examination, and baseline ECGs were available in all the referred patients. Patients with confirmed Brugada syndrome diagnosis were included in the San Donato Brugada Syndrome (BrS) Registry, now including about 1,500 patients. Definitions used to define Brugada patterns were derived from the latest Brugada Consensus Document [4]. Full details of the rationale and design of the BrS registry have been previously published [1,7,8]. The BrS Registry protocol was reviewed and approved by the local Institutional Review Board, and all participants provided written informed consent [7,8].

Brugada Patients

The Brugada patient group included 15 patients with spontaneous type-1 Brugada pattern (mean age 40+9 years, 100% males), and 18 patients with suspicious type 2 or 3 Brugada pattern at baseline who developed type-1 Brugada pattern during Ajmaline provocative test (Ajmaline positive BrS patients, 40+9 years, 80% males). Their baseline and after Ajmaline ECG tracings were included in this analysis. All the included 33 BrS patients had previously undergone an electro-physiologic testing (EPS), had resulted inducible for sustained ventricular arrhythmias, and received an ICD implantation. Most of these patients had a previous history of syncope or cardiac arrest (49%), and most patients had a familial history of unexplained juvenile sudden death (63%). These proportions were not significantly different between spontaneous and Ajmaline-induce BrS patients. All the included BrS patients were studied prior to the acquisition

6

of invasive epicardial mapping prior to epicardial ablation for BrS substrate [7, 8], and their epicardial duration maps were used for the correlation with the *Cine*ECG.

Ajmaline-Negative Patients.

The Ajmaline-negative patient group included 17 patients who underwent a clinical work-up at our Hospital for suspicious type 3 Brugada pattern at baseline, but did not develop a type-1 pattern during Ajmaline test (Ajmaline-negative patients, mean age 36 ± 15 years, 30% males). Both baseline and after Ajmaline ECG tracings were included in the analysis. A familial history of Brugada Syndrome was present in 88% of those patients, a familial history of juvenile sudden death in 16%, none had a previous history of cardiac arrest, and 12% had previous history of unexplained syncope.

All ECG tracings recorded in BrS patients were collected by a customized electrode placement system, optimized for the detection of the BrS pattern, as shown in Figure 1, panel a [7, 8]. The ECG tracings were acquired in digital format by the Workmate Claris™ system of Abbot-St. Jude. In BrS patients (spontaneous and Ajmaline-induced), the 12-ECG tracings utilized in this study were obtained in concomitance with the procedure of acquisition of the combined endo-epicardial mapping (see below).

Control ECG Tracings

As reference for normal or right bundle branch block (RBBB) QRS activation, we utilized the digital ECG tracings derived from the certified Physionet PTB Diagnostic ECG Database https://www.physionet.org/content/ptbdb/1.0.0/ [13], and ECG tracings selected from our San Donato Hospital out-patient clinic, recorded in digital format by Mortara Scribe ECG system. All normal and RBBB tracings were obtained with the standard electrode placement system. All ECG tracings were manually reviewed by two expert cardiologists (EL and GC). A total of 65

7

ECG tracings were included as controls for this study, from 47 normal subjects (mean age 43+15 years, 75% males) and 18 patients with complete RBBB (mean age 69+15 years, 72% males).

iECG Methodology

In order to quantify the cardiac activation pathway, we used the inverse ECG (*iECG*) method, previously described [11]. The cardiac activation pathway of the ventricles represents the average position of all electrically active myocardial tissue during the QRST complex. To construct the cardiac pathway, also referred to as the mean temporal spatial isochrone (mTSI), a model of the ventricles is required in combination with the electrodes positioned on the thorax. For this analysis, we utilized a standard thorax/heart model (Figure 1, panel a), to correlate the cardiac activation pathway to the cardiac anatomy. From this torso/heart model, the *iECG* method computes the vectorcardiogram (VCG) from the recorded 12-lead ECG, taking into account the electrode positions on the thorax, and providing the mean direction of cardiac activation over time (Figure 1, panel a). The mean temporal spatial isochrone (*m*TSI), derived from the VCG, represents the mean trajectory of the cardiac activation pathway, with the mid left septum as starting point (Figure 2). The *m*TSI is used to determine the progression of the cardiac activity to specific areas of the cardiac anatomy, such as the right or left chambers, or the RVOT, and the moving trajectory of the *m*TSI was defined as C*ine*ECG.

QRST Definitions

For each 12-lead ECG tracing, the QRS duration and the *m*TSI derived parameters were computed from a single representative QRS complex. The QRS onset and offset, and the T wave offset were automatically determined from the root mean square (RMS) of the ECG signals (Figure 1, panel b). The QRS onset was determined as the point where the QRS amplitude started to increase steadily from baseline for at least 10 ms. The QRS offset was defined as the first

8

point with the lowest amplitude of the RMS signal occurring between 80 -200 ms after the onset.

The T-wave offset was defined as the time-axis intersection point of the line defined by the T-wave peak with the mid of the downslope T-wave (Figure 1, panel b). Noteworthy, in most cases of normal and RBBB tracings, the QRS offset can be reliably determined. For BrS tracings, the QRS offset is more difficult to be objectively defined. To overcome such difficulty, we introduced three additional time markers, relative to the terminal QRS electrical activity: 1) *QRS90*, i.e. the QRS at 90 ms after the QRS onset, representing the cut-off for a normal QRS duration, 2) the *J-point30*, defined as the QRS offset *(determined as the minimal RMS voltage)* plus 30 ms, and 3) the *Ω-point*, calculated from the intersection of the upslope of the T-wave with the time-axis (the same method used for the T wave downslope, see Figure 1b).

Mean Temporo-Spatial Isochrone (mTSI)

The *m*TSI, which represents the mean trajectory of the cardiac activation pathway, was defined to move through the heart with a constant velocity of 0.7 meter per second (m/s) in the **3D** direction indicated by the VCG $\overrightarrow{(VCG)}$. The velocity of 0.7 m/s is in the physiological range of the myocardial propagation velocity [14, 15]. In detail: The $\overrightarrow{VCG}$, the direction of activation, is computed from the 9 electrodes, building the 12-lead ECG by the following equation:

$$\overrightarrow{VCG}(t) = \sum_{el=1}^{9} ecg_{el}(t) \cdot \alpha_{el} | r_{el} - mTSI(t-1)| \qquad eq.1$$

where $| r_{el} - mTSI|$ is the normalized vector between the *m*TSI 3D-position in the heart and the electrode position on the thorax (r_{el}). The $ecg_{el}(t)$ is the value of the ECG at an electrode at time-sample t. Factor α_{el} was set to 0 for the x direction and 2 for the *y* and *z* directions for the unaugmented extremity leads (VR, VL, and VF). For all other leads, the α_{el} factor was set to 1 for all directions. This formula takes into account and corrects for the two different electrode

9

placement systems utilized for BrS patients and control ECG tracings. The movement of the mTSI is now defined by the direction of the VCG and the previous mTSI position and a propagation velocity v. The mTSI position for t > 0 (=QRS onset) is defined by the following equation:

$$mTSI(t) = mTSI(t-1) + v\frac{VCG(t)}{\|VCG(t)\|} \qquad eq.2$$

In this study, all patients being in normal sinus rhythm, the cardiac activation starts in the left septum, close to the center of mass of the ventricles [16, 17]. Thus, the center of mass of the ventricular model is used as the $mTSI(0)$ starting point. The mTSI is relatively insensitive to noise in the ECG/VCG, because it uses only the direction of the VCG and not its amplitude. No additional signal processing on the mTSI is therefore required. Moreover, the computation of the Cine-ECG is almost instantaneous (< 200ms) enabling its use also while recording the ECG.

CineECG Definitions

In order to visualize the tempo-spatial localization of the electrical activity pathway, we introduced the new concept of "*Cine*ECG", representing the moving trajectory of the mTSI within the cardiac anatomic structures. To establish and visualize a quantifiable relation between the cardiac anatomy and the mTSI trajectory, three standard X-ray views on the heart were created from the heart model: a standard 4-chamber view, and right and left anterior oblique views (RAO and LAO, Figure 2). Therefore, the terminal direction of the mTSI can be related to specific structures of the heart, like septum, and RV or LV free walls, or RVOT. An example of the construction and visualization of the VCG and mTSI for a normal activation is shown in Figure 2 and web-movie 1. In a normal subject, the $\overrightarrow{VCG}$ is mainly pointing towards the LV free wall, with a small initial trans-septal vector. In the mTSI trajectory, the trans-septal vector is clearly visible. Moreover, the mTSI stays close to the septum ending in the mid-base LV area.

10

CineECG Parameters

In order to quantify the cardiac activation pathway depicted by the *Cine*ECG, new quantitative parameters derived from mTSI were also defined:

- **Trans-cardiac ratio (TCR):** The trans-cardiac ratio (TCR) is defined as the 3D-distance between the starting and the ending points of the mTSI, coincident with the QRS onset to the QRS offset. As this measure is potentially influenced by the size of the heart, it is weighted by the size of the heart model, resulting as a relative number. From our previous experience, normal cardiac activation is usually associated with a trans-cardiac ratio generally well below 40% 11. As an example, the trans-cardiac ratio for the normal subject shown in Figure 2 was 11%.

- **mTSI Spatial Location:** At each time sample of the *m*TSI, its 3D-spatial localization in the heart is determined, and three cardiac areas were defined, either septal, left ventricle (LV), or right ventricle (RV). The initial spatial location of the *m*TSI is left septal, and it moves according to the direction determined by the VCG. In case of normal activation, the *m*TSI initially moves trans-septal and then towards the LV, staying close to the septum (Figure 2). The spatial location is computed as the percentage of QRS duration spent by the *m*TSI in each of the three cardiac areas. As an example, in a normal subject, the *m*TSI is located for 55% of the QRS duration in the septum, for 45% in the LV, but never in the RV (Figure 2).

- **Terminal mTSI direction:** In order to measure the direction of the electrical activity occurring during the terminal phase of the QRS, or concealed within the ST segment, we computed the location of the terminal *m*TSI direction at the three time markers related to the end of QRS electrical activity as described above, i.e. QRS90, J-point30, and Ω-point

11

(Figure 1, panel b). The terminal mTSI direction is quantified as a relative number between -1 and +1, indicating the congruence with the direction of any of the three cardiac axes (Figure 2).

- **mTSI Classification Algorithm:** Based on the QRS duration and on the above described mTSI parameters, a classification algorithm was developed to test the ability to discriminate tracings with spontaneous or Ajmaline-induced type-1 BrS pattern from normal or RBBB tracings. Four diagnostic classes were defined: 1) *"Normal"*, 2) *"RBBB"*, and 3) *"Brugada"*, 4) *"Undetermined"*. For each class, a set of parameter values were used to compute the probability of a certain classification. The probability for a certain parameter is set to either 0 or 1, with 1 indicating the classification met, and 0 the classification not met. The classification was determined by the highest probability score. The following criteria were used to :

  "Normal": QRS duration < 110 ms, TCR 5-38%, terminal *m*TSI direction towards the LV basal area.

  "RBBB": QRS duration 120-190 ms, TCR >50%, terminal *m*TSI towards RV basal area

  "Brugada": QRS duration > 110 ms, TCR >50%, terminal *m*TSI, specifically defined for BrS between 110 and 180 ms after onset QRS, towards the RV free wall or RVOT (NOT towards the RV or LV basal area).

  "Undetermined": Did not match any of the criteria above.

Electrophysiological epicardial mapping

All Brugada patients underwent a combined endo-epicardial mapping procedure using a three-dimensional (3D) mapping system (CARTO 3, Biosense Webster, CA, USA), as previously

12

described [7, 8]. All maps were obtained at baseline conditions and after drug challenge (Ajmaline up to 1mg/kg in 5min). Total signal duration was measured for each potential before and after drug challenge as previously described [7, 8]. Measurements were interpreted and validated online by two expert electrophysiologists using the CARTO3 system electronic caliper. The potential duration map (PDM) was created by collecting the duration of each EGM. As a result, a color-coded map was obtained showing the regions displaying the shortest (red color) and the longest (purple color) durations. The electrical substrate area was defined as an area where abnormal electrograms (EGMs) were identified, if they met at least one of the following characteristics: (i) a wide duration (>110ms) with fragmented component (>3 distinct peaks); (ii) late component of low voltage amplitude ranging from 0.05 to 1.5mV; (iii) distinct and delayed component exceeding the end of the QRS complex [7, 8].

Statistical methods

Statistical analysis was conducted using the software IBM SPSS 1.0.0.1327. CineECG parameters, including QRS duration, trans-cardiac ratio, mTSI Spatial Location (septal, left ventricle (LV), or right ventricle (RV)), and terminal mTSI directions (at each of the three time markers, end of QRS electrical activity QRS90, J-point30, and Ω-point), were compared among the seven sample groups: Normal, RBBB, Spontaneous Brugada pattern type 1, Ajmaline-Induced Brugada Patients (at baseline and after Ajmaline) and Ajmaline-Negative Patients (at baseline and after Ajmaline).

Data were assessed using Shapiro Wilk (p<0.05), normality plots and box plots. The null hypothesis of normal distribution was rejected for all the parameters (p<0.001). Data were provided as means, with 95% upper and lower confidence intervals. The Kruskal-Wallis 1-way ANOVA for nonparametric data was therefore used to perform pairwise comparison between the

13

different ECG diagnostic groups. The Bonferroni P value adjustment was applied to correct for multiple comparisons. Probability values less than 5% were considered significant.

Results

In Table 1, we provide the quantitative results for all study groups for the *Cine*ECG parameters, specifically the mean QRS duration, the mTSI spatial location, the trans-cardiac ratio (TCR), and the location of the terminal mTSI direction (from QRS90 to QRS offset). The full results of the statistical analysis are provided in the online Supplemental Material.

Normal Subjects

For the 47 normal subjects, the QRS duration was on average 90 ms (Table 1). The mTSI direction was generally pointing towards the LV basal area, and the *m*TSI trajectory was compact, resulting in a TCR with a median value of 23% (Figure 3, panel a). The *Cine*ECG illustrated the trajectory of the mTSI across the heart, showing an initial trans-septal vector, then moving to the left chamber (web material Movie 1). Only three out of the 47 normal subjects (6%) had a trans-cardiac ratio of more than 40%, which is considered large for an activation initiated by the His-Purkinje system (Figure 2). They partially overlapped the features of the RBBB and Brugada ECG patterns, although their QRS were less than 110 msec, and their terminal mTSI location was still in the left chamber. Among normal subjects, the *Cine*ECG classification came to a correct adjudication as "N*ormal"* in 44 out 47 cases (94%): In three cases, all with larger than average TCR ratio the classification was "U*ndetermined"* (Table 2).

RBBB Patients.

For the 18 RBBB patients, the QRS duration was on average 144 ms (Table 1), significantly longer than normal subjects and Ajmaline-negative patients, but not significantly different from

14

spontaneous and Ajmaline-induced BrS patients. The median TCR value was 36%, and the *Cine*ECG generally showed an open loop configuration (Figure 3, panel b). As to the terminal mTSI in the four chamber and RAO projections, there was no overlapping between normal subjects and RBBB patients.

Their *Cine*ECG showed an initial trans-septal vector, then moving towards the RV basal area, representing an activation going from the right apical region towards the right base of the heart (web material movie 2). According to the *Cine*ECG classification, all patients with RBBB on standard 12-lead ECG were correctly adjudicated as "*RBBB*".

Spontaneous Type-1 Brugada Patients.

In the 15 patients with spontaneous type-1 Brugada pattern, the QRS duration was on average 154 ms, and the median TCR was 26%, with an open loop configuration (Table 1). This was significantly higher than normal subjects, but not different from RRBB patients. Noteworthy, at a difference with normal and RBBB tracings, in spontaneous BrS patients, the terminal *m*TSI direction was homogeneously directed towards the RVOT (Table 1, Figure 3, panel c, and web material Movie 3).

The RVOT localization of the mTSI terminal activation detected by *CineECG* was congruent with the area of arrhythmogenic substrate detected by the PDMs (see Figure 4, panel a). All spontaneous BrS patients were correctly adjudicated to the "*Brugada*" classification (Table 2).

Ajmaline-Induced Brugada Patients

In the 18 Ajmaline-induced BrS patients, the QRS duration was 122 ms at baseline and significantly increased to 156 ms (Table 1). The mTSI always had an open loop configuration,

15

and the terminal *m*TSI direction was homogeneously directed towards the RVOT. Type-2 BrS pattern was present in 5 patients, while type-3 BrS pattern in the remaining 13 patients.

In Ajmaline-induced BrS patients, the only significant difference between baseline and after Ajmaline parameters was in the QRS duration, while all *Cine*ECG parameters were in the same range, and specifically, the terminal *m*TSI direction was mainly and homogeneously already directed towards the RVOT even at baseline (Table 1, Figure 5, panels a and b, and web material Movie 4 and 5). The mean spatial direction of the terminal mTSI, in the four chamber and RAO projections, had a similar behavior both in spontaneous and Ajmaline-induced BrS patients.

No significant differences between spontaneous or Ajmaline-induced Brugada patients in most *Cine*ECG parameters were observed. In both groups, the RVOT localization of the mTSI terminal activation by *CineECG* was congruent with the area of arrhythmogenic substrate detected by the epicardial PDMs after Ajmaline infusion (see Figure 4, panel b, and web material Movie 5).

Noteworthy, by the *Cine*ECG method, 78% of the baseline ECG tracings of Ajmaline-induced BrS patients was already correctly classified as "*Brugada*", and the remaining were classified either as "*Normal*" or "*Undetermined*". After Ajmaline, 100% were classified as "*Brugada*".

Ajmaline-Negative Patients

In the 17 patients, all with type 3 Brugada pattern at baseline, who did not develop a typical type-1 Brugada pattern on the standard 12-lead ECG after Ajmaline infusion (Ajmaline-negative patients), the QRS duration was 100 ms at baseline and significantly increased to 121 ms after Ajmaline (Table 1, Figure 5, panel c and d). According to the *Cine*ECG parameters, none of

these patients showed a RVOT localization of the mTSI terminal activation at baseline, so none was classified as "*Brugada*", and all were classified as "*Normal*" or "*Undetermined*". After Ajmaline infusion, heterogeneous patterns were revealed by the *Cine*ECG, since 41% were classified as "*Normal*", 6% were classified as "*RBBB*", 35% were "*Undetermined*", and 18% were classified as "*Brugada*" (Table 2).

Discussion

Our novel *CineECG* method, developed from the mean temporo-spatial isochrones derived from standard 12-lead ECG tracings, by combining ECG data with the cardiac anatomy, created a direct relation between the electrical signals and their anatomical cardiac sources. Our main finding was that the *CineECG* method showed that the temporo-spatial localization of the abnormal BrS activation is pointing towards the RVOT. This unique feature was observed both in spontaneous and in Ajmaline-induced type-1 BrS patients (both at baseline and during Ajmaline), but it was never observed in normal subjects, nor in RBBB patients, nor in Ajmaline-negative patients at baseline.

The possibility to identify the RVOT location by our novel non-invasive *Cine*ECG, based on the elaboration of the readily available standard 12-lead ECG, opens an entirely new horizon for improving the diagnosis of BrS patients. So far, the specific localization of the terminal QRS forces in the RVOT in BrS patients could only be demonstrated by complex mapping methods, either by body surface mapping, requiring the acquisition of 250 electrodes [6], or by invasive epicardial isopotential mapping [7, 8].

17

Interpretation of the *Cine*ECG

The trajectory of the mTSI represents the position of the average electrical forces at any given moment during the QRS, in relation with their cardiac sources. In normal subjects, the two ventricles are activated almost simultaneously, resulting in mTSI mainly located in the septal and left ventricular area (Figure 3, panel a, and web material movie 1). In patients with RBBB, the initial forces are located in the left septum and in the left ventricle, while the terminal mTSI was directed towards the right ventricular base (Figure 3, panel b and web material movie 2). In patients with both spontaneous and Ajmaline-induced type-1 BrS pattern, at baseline and after Ajmaline, the initial forces are located in the left septum and in the left ventricle, while the terminal mTSI is univocally directed towards the RVOT (Figure 3, panel c, Figure 4, panel a and b, and web material movies 3, 4 and 5). This typical behavior was already present at baseline in 78% of Ajmaline-induced patients, in whom type-2 (in 5 cases) or type-3 Brugada pattern was present on the standard 12-lead ECG tracing.

The *Cine*ECG method, computed from standard 12-lead ECG, was able to show the same RVOT localization in BrS patients, that was demonstrated by body surface mapping (BSM) requiring 250 electrodes [6], or by invasive epicardial isopotential mapping [7, 8]. The *Cine*ECG method, at a difference with scalar ECG and BSM can also show the dynamic behavior of the mTSI within the heart model, correlating the cardiac electrical activity with its sources. Therefore, this method can improve the interpretation of the ECG waveforms and may open new horizons for the diagnostic and prognostic value of the standard 12-lead ECG. Possible clinical applications, besides the BrS, may be the localization of accessory pathways, the interpretation of intraventricular conduction disorders, the evaluation of the resynchronization therapies, and maybe the localization of acute myocardial infarction.

18

Electrophysiologic basis of *Cine*ECG

The CineE*CG* method provides the temporo-spatial trajectory of the summed electrical gradients, which may be due either to the activation or to the recovery process. Thus, the CineE*CG* method cannot discriminate whether any terminal *m*TSI pathway is due either to a local slowing of the activation velocity or to early start of the ventricular recovery process.

More specifically, our results indicate that all BrS patients had predominant electrical forces pointing towards the right ventricular outflow tract in the period corresponding to the terminal portion of the QRS and the initial phase of the ST segment. However, this method cannot discriminate whether this phenomenon was due to endo-to-epicardial activation delay, or to epi-to-endocardial early recovery forces. Further investigation, with more precise spatial reconstructions, may improve the understanding of the patho-phsysiologic mechanisms related to the *Cine*ECG model.

Congruence of RVOT Localization by *Cine*ECG and Epicardial Potential Duration Maps

In BrS patients, the 12-ECG tracings utilized for this study were obtained in concomitance with the procedure of acquisition of the combined endo-epicardial mapping. In both spontaneous and Ajmaline-induced BrS patients, the epicardial potential duration mapping (PDM) identified the location of the electrical substrate area in RVOT or RV anterior wall, concordant with the location of the terminal mTSI forces in RVOT, as illustrated by the *Cine*ECG (Figure 4, panels a and b). Therefore, the *Cine*ECG can be viewed as a new non-invasive mapping system, that may identify the presence and the anatomical location of the arrhythmogenic substrate in BrS patients. This finding opens new perspectives for the diagnostic and prognostic evaluation of BrS patients. In this view, a very promising new finding is the detection of the typical RVOT already present

19

at baseline in the majority of Ajmaline-induced BrS patients, where the standard 12-lead ECG only showed non-diagnostic type-2 or -3 pattern.

Comparison between *Cine*ECG and standard 12-lead ECG

Noteworthy, the *Cine*ECG already classified as "Brugada" 78% of the Ajmaline-positive patients, who only had non diagnostic type 2 or type 3 pattern on baseline ECG. In contrast, none of the Ajmaline-negative patients was classified as "Brugada". Therefore, at a difference with the standard 12-lead ECG, the *Cine*ECG obtained at baseline had high positive predictive value (100%) and negative predictive value (81%) in predicting the result of the Ajmaline test. These results suggest that the novel noninvasive *Cine*ECG method, derived by a digital standard 12-lead ECG, may guide and limit the need to perform the Ajmaline test. Notwithstanding these promising results, further studies, with a much higher number of patients, are required to determine the precise diagnostic value of the novel *Cine*ECG in detecting BrS.

Limitations

In this study, we used the standard heart/torso model to obtain the direct projection of the *m*TSI to the cardiac anatomy, (Figure 1). In this study, the 12-lead ECGs of BrS patients and controls were obtained with two different electrode placement configurations, and the *Cine*ECG method automatically corrected for the electrode position (see Equation 1 and Figure 1) [11]. As future development, to take into consideration differences in individual thorax size and heart orientation, and to better localize the precise ECG electrode placement on the torso, we plan the use of a 3D camera to implement the thorax conformation into the algorithm and. This may increase the accuracy of temporo-spatial localization of the *Cine*ECG waveforms [18].

Although the consistency of the *Cine*ECG behavior in each patient group supports the proof-of-concept and robustness of our method, further studies will be needed to confirm these

20

results, preferably with a method utilizing a personalized heart/torso model with customized electrode positions.

Conclusions

The novel *CineECG* method, starting from the standard 12-lead ECG tracing, computes the mean temporo-spatial isochrone, combining ECG data with the cardiac anatomy. This new *Cine*ECG was able to localize the late QRS electrical activity to RVOT in patients with BrS, both in spontaneous type-1 BrS pattern and in Ajmaline-induced type-1 BrS pattern (both at baseline and after Ajmaline), congruent with the anatomical localization of the arrhythmogenic substrate by the epicardial isopotential maps. A late QRS electrical activity to RVOT was observed neither in normal subjects nor in patients with RBBB or Ajmaline-negative patients at baseline. The *CineECG*, derived from standard 12-lead ECG, can improve the understanding of the temporo-spatial localization of the electrical waveforms, thus may increase the diagnostic and prognostic accuracy of the standard 12-lead ECG not only in BrS, but also in other cardiac arrhythmogenic diseases.

References:

1. Pappone C, Santinelli V. Brugada Syndrome: Progress in Diagnosis and Management. *Arrhythm Electrophysiol Rev.* 2019;8:13-18.

2. Priori SG, Blomstrom-Lundqvist C, Mazzanti A, Blom N, Borggrefe M, Camm J, Elliott PM, Fitzsimons D, Hatala R, Hindricks G, et al. 2015 ESC Guidelines for the Management of Patients with Ventricular Arrhythmias and the Prevention of Sudden Cardiac Death. *Rev Esp Cardiol (Engl Ed)*. 2016;69:176.

3. Antzelevitch C, Patocskai B. Brugada Syndrome: Clinical, Genetic, Molecular, Cellular, and Ionic Aspects. *Curr Probl Cardiol*. 2016;41:7-57.

4. Kapplinger JD, Tester DJ, Alders M, Benito B, Berthet M, Brugada J, Brugada P, Fressart V, Guerchicoff A, Harris-Kerr C, et al. An international compendium of mutations in the SCN5A-encoded cardiac sodium channel in patients referred for Brugada syndrome genetic testing. *Heart Rhythm*. 2010;7:33-46.

5. Gottschalk BH, Anselm DD, Brugada J, Brugada P, Wilde AA, Chiale PA, Perez-Riera AR, Elizari MV, De Luna AB, Krahn AD, et al. Expert cardiologists cannot distinguish between Brugada phenocopy and Brugada syndrome electrocardiogram patterns. *Europace*. 2016;18:1095-100.

6. Zhang J, Sacher F, Hoffmayer K, O'Hara T, Strom M, Cuculich P, Silva J, Cooper D, Faddis M, Hocini M, et al. Cardiac electrophysiological substrate underlying the ECG phenotype and electrogram abnormalities in Brugada syndrome patients. *Circulation*. 2015;131:1950-9.

7. Chevallier S, Forclaz A, Tenkorang J, Ahmad Y, Faouzi M, Graf D, Schlaepfer J, Pruvot E. New Electrocardiographic Criteria for Discriminating Between Brugada Types 2 and 3 Patterns and Incomplete Right Bundle Branch Block. *J Am Coll Cardiol*. 2011;58:2290-2298.

8. Serra G, Baranchuk A, Bayes-De-Luna A, Brugada J, Goldwasser D, Capulzini L, Arazo D, Boraita A, Heras ME, Garcia-Niebla J, et al. New electrocardiographic criteria to differentiate the Type-2 Brugada pattern from electrocardiogram of healthy athletes with r'-wave in leads V1/V2. *Europace*. 2014;16:1639-45.

9. Pappone C, Ciconte G, Manguso F, Vicedomini G, Mecarocci V, Conti M, Giannelli L, Pozzi P, Borrelli V, Menicanti L, et al. Assessing the Malignant Ventricular Arrhythmic Substrate in Patients With Brugada Syndrome. *J Am Coll Cardiol*. 2018;71:1631-1646.

10. Pappone C, Mecarocci V, Manguso F, Ciconte G, Vicedomini G, Sturla F, Votta E, Mazza B, Pozzi P, Borrelli V, et al. New electromechanical substrate abnormalities in high-risk patients with Brugada syndrome. *Heart Rhythm*. 2020;17:637-645.

11. Van Dam PM. A new anatomical view on the vector cardiogram: The mean temporal-spatial isochrones. *J Electrocardiol*. 2017;50:732-738.

12. Roudijk R, Loh KP, van Dam PM. Mean Temporal Spatial Isochrones Direction as marker for Activation Delay in Patients with Arrhythmogenic Cardiomyopathy. *Comput Cardiol*. 2018;45:1-4.

22

13. Bousseljot R, Kreiseler D, Schnabel A. Nutzung der EKG-Signaldatenbank CARDIODAT der PTB über das Internet. *Biomedizinische Technik / Biomedical Engineering.* 1995:317-318.

14. Kléber AG, Janse MJ, Wilms-Schopmann FJ, Wilde AA, Coronel R. Changes in conduction velocity during acute ischemia in ventricular myocardium of the isolated porcine heart. *Circulation.* 1986;73:189-198.

15. Roberts D, Hersh L, Scher A. Influence of cardiac fiber orientation on wavefront voltage, conduction velocity, and tissue resistivity in the dog. *Circ Res.* 1979;44:701-712.

16. Durrer D, van Dam RT, Freud GE, Janse MJ, Meijler FL, Arzbaecher RC. Total excitation of the isolated human heart. *Circulation.* 1970;41:899-912.

17. Van Dam PM, Oostendorp TF, Linnenbank AC, van Oosterom A. Non-invasive imaging of cardiac activation and recovery. *Ann Biomed Eng.* 2009;37:1739-1756.

18. Van Dam PM, Gordon JP, Laks M. Sensitivity of CIPS-computed PVC location to measurement errors in ECG electrode position: the need for the 3D Camera. *J Electrocardiol.* 2014;47:788-793.

Table 1: CineECG Characteristics per patient group (mean, 95% confidence interval)

Patient Groups	# Pts	Test type	QRS duration ms	TCR %	mTSI spatial location %			Terminal mTSI direction	
					Septum	LV	RV	to RVOT	to base
Normal subjects	47	**Baseline**	90 (88/92)*†‡	23 (3-53)*	79 (45-100)†	21 (0-55)*	0 (0-3)*†	0.07 (-0.06/0.21)†§	-0.52 (-0.71/-0.33)*†‡
RBBB patients	18	**Baseline**	144 (135/152)*§‖	36 (31-59)*§‖	68 (43-100)	0 (0-44)*	22 (0-42)*§‖	0.03 (-0.05/0.12)	0.58 (0.39/0.78)*§
Spontaneous Brs patients	15	**Baseline**	154 (137/171)†	26 (14-55)	68 (21-100)†	7 (0-63)	0 (0-79)†§	0.58 (0.38/0.79)†§	0.10 (-0.04/0.24)
Ajmaline-positive BrS patients	18	**Ajmaline**	156 (146/166)†	29 (12-47)	74 (23-100)	0 (0-77)	3 (0-54)†§	0.64 (0.36/0.92)†§	0.24 (0.08/0.40)†
		Baseline	122 (115/130)†	24 (16-39)§	72 (39-100)	21 (0-62)	0 (0-50)§	0.4 (0.06/0.74)	-0.16 (-0.38/0.07)§
Ajmaline-negative patients	17	**Ajmaline**	121 (110/131)‡	26 (10-44)‖#	72 (19-100)	24 (0-64)	0 (0-81)‖	0.4 (-0.01/81)	0.25 (-0.4/0.53)‡
		Baseline	100 (93/107)‖	16 (4-51)‖#	83 (20-100)	15 (0-80)	0 (0-64)‖	0.42 (0.12/0.72)	0.12 (-0.14/0.39)‡

The descriptive statistics for every patient group of the QRS duration (mean and 95 % confidence interval in ms), the trans-cardiac ratio (TCR, median and the range (minimum-maximum) in %), mTSI spatial location (median and the range (minimum-maximum) in %), and terminal mTSI direction quantified, all given as a relative number between -1 and +1 (mean and 95 % confidence interval) (see text for definitions). The Kruskal-Wallis 1-way ANOVA for nonparametric data was used to perform pairwise comparison between the different ECG diagnostic groups. The Bonferroni P value adjustment was applied to correct for multiple comparisons. Significant differences (p value <0.05) for each comparison was indicated as follows:

*comparison between normal subjects vs. RBBB patients

†normal subjects vs. either spontaneous or Ajmaline-induced (baseline and after Ajmaline) patients

‡normal subjects vs. non-inducible patients (baseline and after Ajmaline)

§RBBB vs. BrS patients, either spontaneous or Ajmaline-induced (baseline and Ajmaline)

‖ RBBB vs. Ajmaline-negative patients (baseline and after Ajmaline)

Baseline vs. after Ajmaline in both for Ajmaline-induced and Ajmaline-negative patients. Noteworthy, no significant differences were observed between Spontaneous BRS and Ajmaline-induced BrS patterns (see online Supplemental Material for further details on the Statistical Analysis).

Table 2: MeanTSI classification accuracy per patient group.

Patient group	Test type	Normal	RBBB	Brugada	Undetermined
Normal subjects (47)	**Baseline**	0.94 (44)	0	0	0.06 (3)
RBBB Pts (18)	**Baseline**	0	1.00	0	0
Spontaneous BrS Pts (15)	**Baseline**	0	0	1.00	0
Ajmaline-Induced BrS Pts (18)	**Baseline**	0.11(2)	0	0.78 (14)	0.11(2)
	Ajmaline	0	0	1.00 (18)	0
Ajmaline Negative Pts (17)	**Baseline**	0.88 (15)	0	0	0.12 (2)
	Ajmaline	0.41 (7)	0.06 (1)	0.18 (3)	0.35 (6)

Classification is given as probability between 0 (no likelihood of diagnosis) and 1.0 (high likelihood of diagnosis). For Normal subjects, RBBB pts, Spontaneous and Ajmaline induced BrS Patients, the likelihood of diagnosis in the correct class was above 0.9 (90%). In three of the 47 normal subjects, the diagnosis was undermined, while all RBBB patients, all the spontaneous BrS patients and all Ajmaline-induced BrS patients were correctly classified as Brugada. Noteworthy, 78% of the baseline tracings of Ajmaline-induced BrS patients, only showing type-2 or 3 BrS pattern, were already correctly classified as Brugada by CineECG parameters. In contrast, the "Brugada" pattern was never observed at baseline in those who were diagnosed as "Ajmaline-negative" based on the standard 12-lead ECG after Ajmaline infusion.

Figure Legends:

Figure 1: Panel a) The torso/heart model used with the 8 of the 9 electrode positions (the VF electrode is not shown). The torso/heart model on the left represents the standard 12 lead ECG configuration, used to analyze the PTB and clinical database ECGs. The torso/heart model on the right shows the model, with the adapted Brugada lead system. Panel b) the fiducials of a single ECG beat from the 12 lead ECG were automatically derived from the root mean square (RMS) of all ECG signals measured. The QRS onset was defined as the time when subsequent ECG samples have an increasing value for at least 10 ms. The QRS offset was defined as the time when the RMS amplitude is lowest between 80 and 200 ms after the detected QRS onset. QRS90 was defined as the time 90 ms after QRS onset. J-Point 30 is defined as the time 30 ms after the QRS offset, and the Ω-point is defined by the intersection point at the time axis and the upslope tangent between the T-peak and the mid- amplitude T-wave (oranges lines). Similarly, the T-wave end is defined by the intersection point at the time axis and the downslope tangent between the T wave peak and the mid T wave amplitude (blue lines)

Figure 2: The CineECG work-flow in a normal subject. The first step is to convert the 12-lead ECG into the VCG, positioned at the center of ventricular mass, from which the mean temporal spatial isochrone (mTSI) trajectory can be constructed (lower panel on the right). The ventricles are projected in three standard orientations: 1) Four chambers, Right Anterior Oblique (RAO) and Left Anterior Oblique views (LAO). The right ventricle is indicated in transparent blue. The blue arrows indicate the Right-to-Left axis (LR-axis), the green arrow the Posterior-to-Anterior axis (PA-axis), and the red arrow the Base-to-Apex axis (BA-axis). The colors of the VCG and

26

mTSI indicate the time from the QRS onset to the QRS offset (color bar on the right). The trans-septal vector is indicated in red. In this case, the trans-cardiac ratio (TCR) is 11%, as the starting point (red) and the end point (purple) are very close. In this case, the mTSI is located for 55% of the QRS duration in the septal region, while for the 45% of the QRS duration in the left ventricle.

Figure 3: Three typical examples of the mTSI trajectory for a normal control (panel a); a RBBB patient (panel b); and a patient with spontaneous Brugada type-1 pattern (panel c). In the spontaneous Brugada BrS patient, the CineECG showed the terminal mTSI location in the RVOT. For each patient, the mTSI is shown by the colored line during the QRS, while the terminal mTSI (including T wave) is shown as a solid grey line, indicating also the terminal direction of the meanTSI during the ST segment. The colors indicate the time during the QRS, red early and purple late.

Figure 4: The epicardial PDMs of one spontaneous BrS patient (panel a) and one Ajmaline-induced BrS patient (panel b). PDMs and 12-lead ECG tracings were obtained simultaneously. The arrhythmogenic substrate area is indicated in purple. In both cases, the locations of the substrate area detected by the PDM and the location of the terminal mTSI by CineECG were coincident, in both cases located in the RVOT area.

Figure 5: Two typical examples of the mTSI trajectory for a patient with Ajmaline-induced Brugada pattern at baseline (panel a) and after Ajmaline (panel b) and an Ajmaline-negative patient at baseline (panel c) and after Ajmaline (panel d). In the Ajmaline-induced BrS patient, the CineECG showed the terminal mTSI location in the RVOT, even if the 12-lead ECG tracing

27

only showed type-2 BrS pattern. For the Ajmaline-negative patient, the CineECG classified

normal at baseline, and RBBB after Ajmaline. The mTSI is shown by the colored line during the

QRS, while the terminal mTSI (including T wave) is shown as a solid grey line, indicating also

the terminal direction of the meanTSI during the ST segment. The colors indicate the time during

the QRS, red early and purple late.

What Is Known?

- In Brugada Syndrome (BrS), diagnosed in presence of a spontaneous or Ajmaline-induced type-1 pattern, ventricular arrhythmias have been shown to originate from the right ventricle outflow tract (RVOT).

- So far, the RVOT localization could only be demonstrated by complex mapping methods, either by body surface mapping requiring the acquisition of 250 electrodes, or by invasive epicardial isopotential mapping.

What the Study Adds?

- The cineECG, derived from 12-lead ECGs by an inverse ECG method, enabled the temporo-spatial localization of the ECG waveforms to a 3D heart model.

- In Brugada patients, the terminal components of the ventricular depolarization were localized to the RVOT, congruent with the localization of the arrhythmogenic substrate detected by epicardial potential duration maps.

- The RVOT localization of the QRS terminal components never occurred in normal subjects and in right bundle branch block (RBBB) patients, while it was present already at baseline in patients who developed type-1 Brugada pattern during Ajmaline infusion.
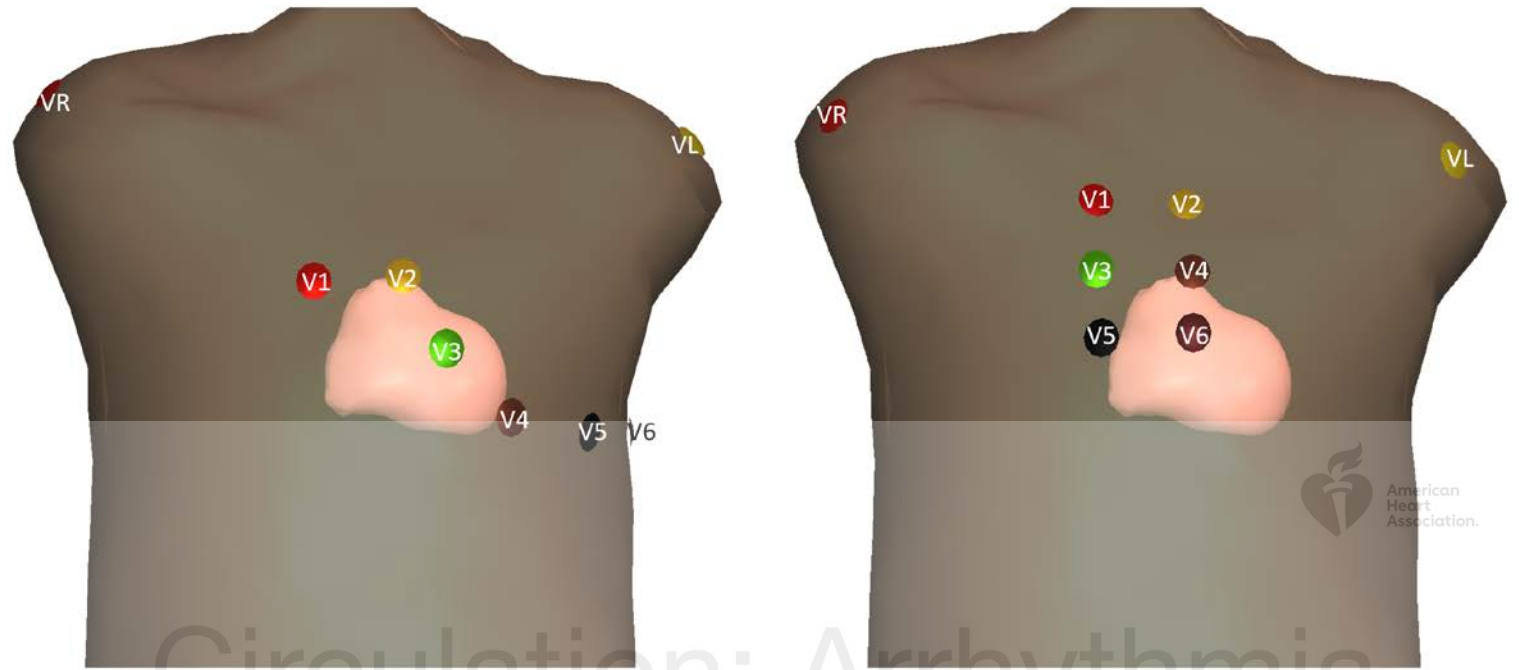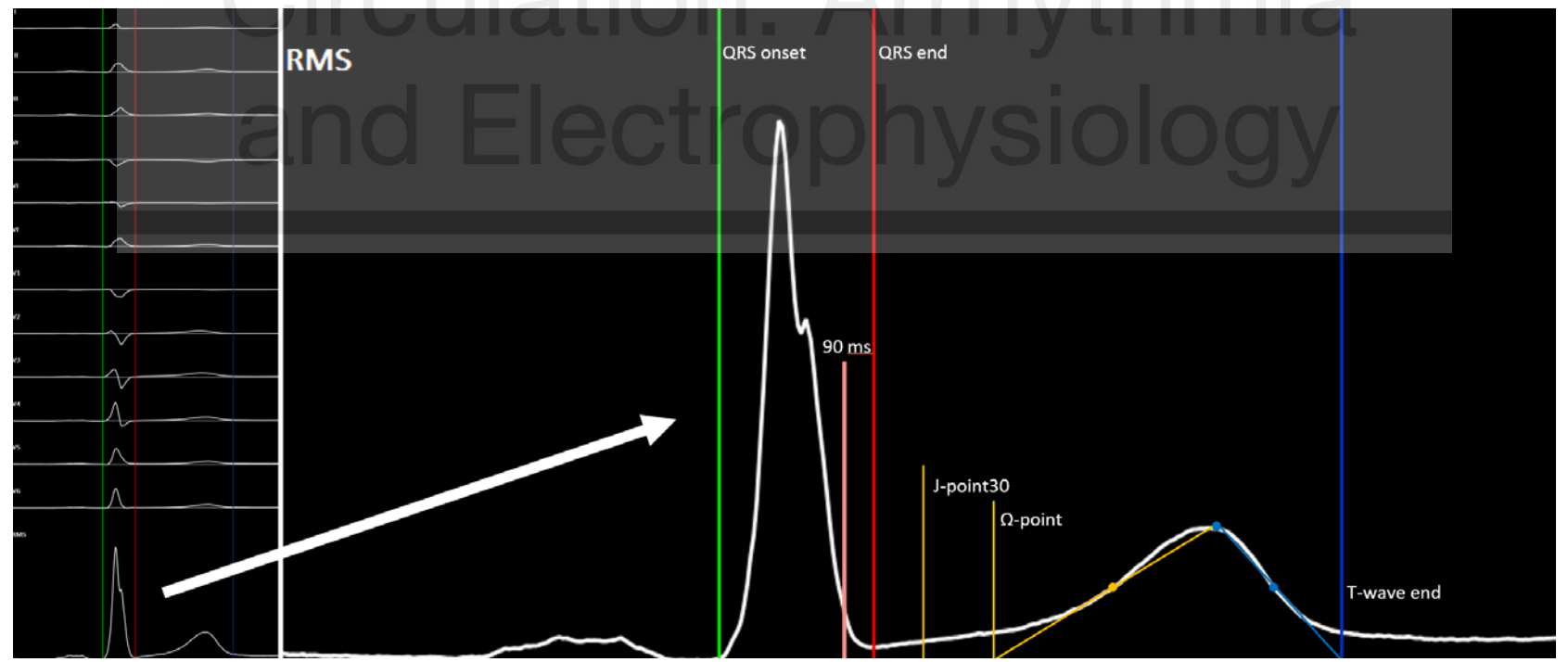
29

Standard 12 lead ECG

ECG to VCG

vectorcardiogram

4 chamber

RAO

LAO
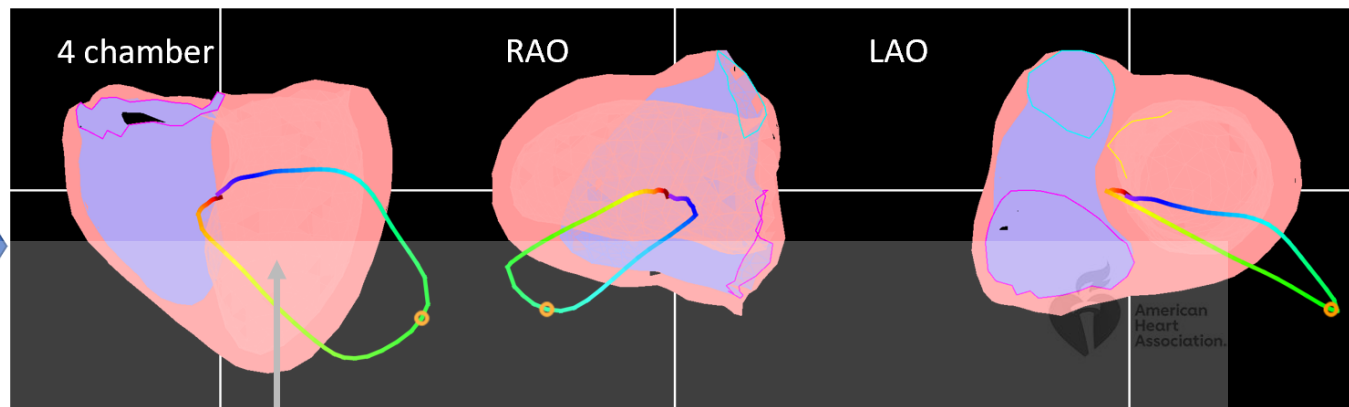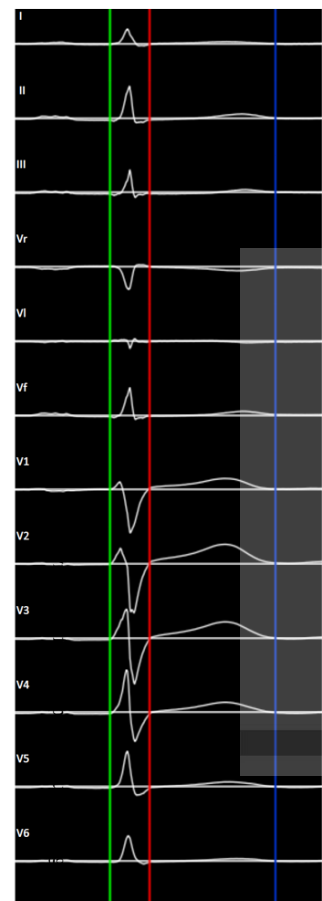
center ventricular mass

VCG to meanTSI

Mean temporal spatial isochrone

ms

80

60

40

20

0

American Heart Association.
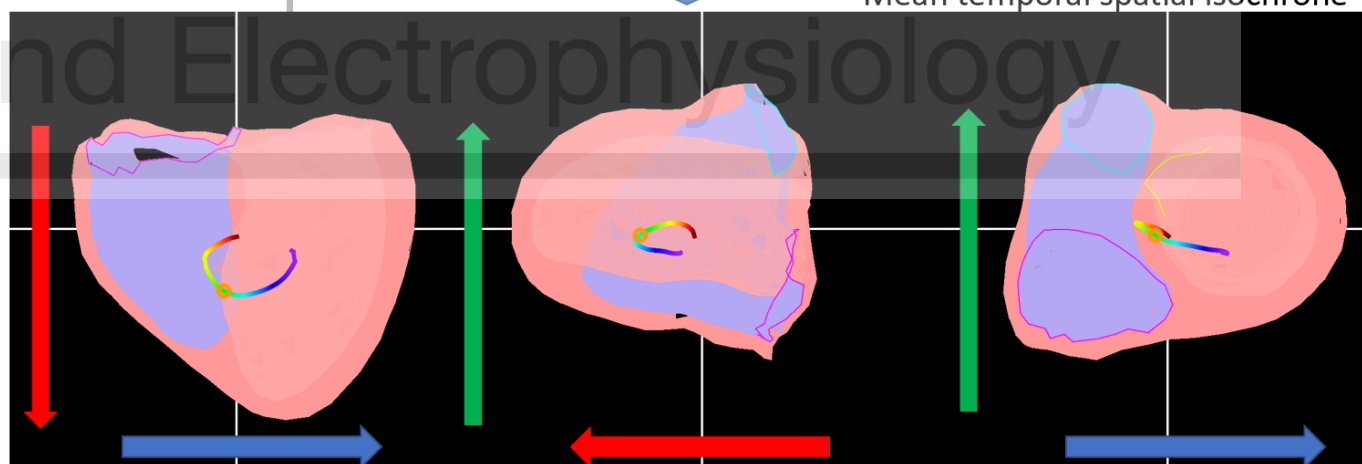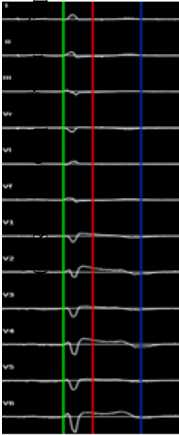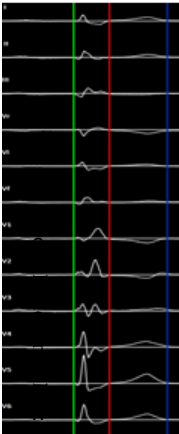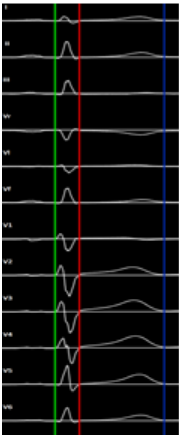
a) Normal

b) RBBB
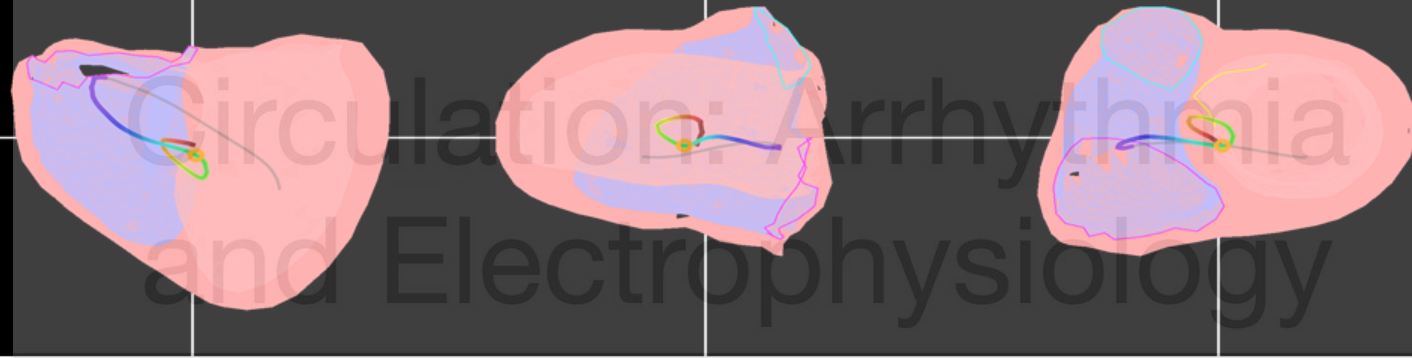
c) Spontaneous Brs
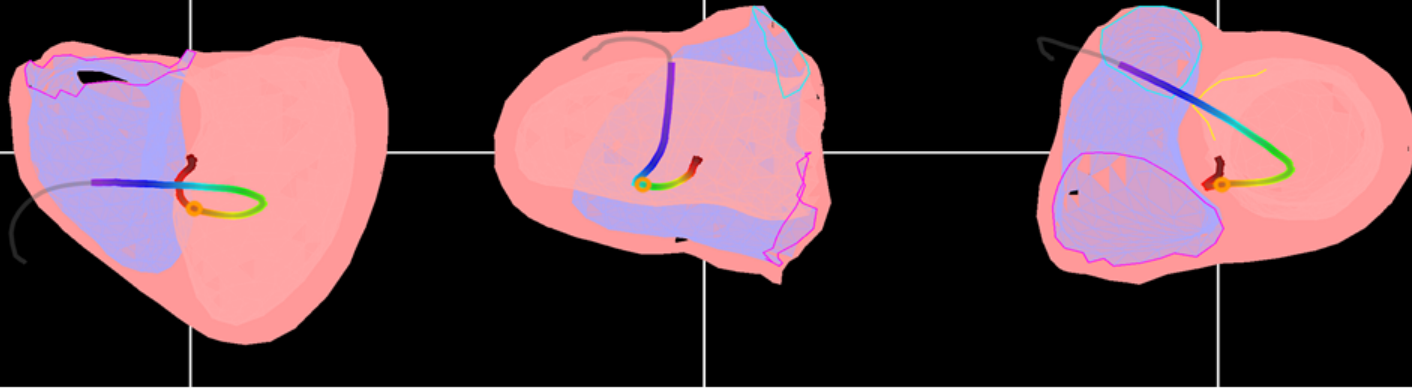
%QRS

80

60

40

20

0

a) Spontaneous Brs

iECG indicated area
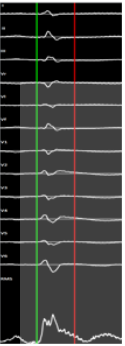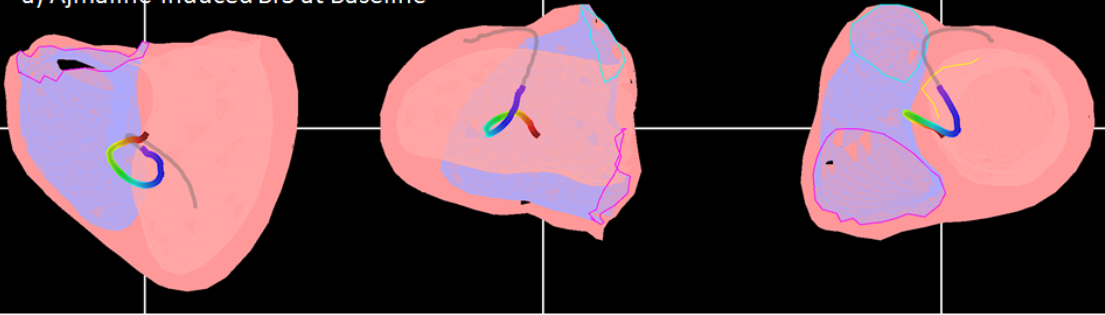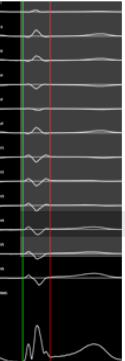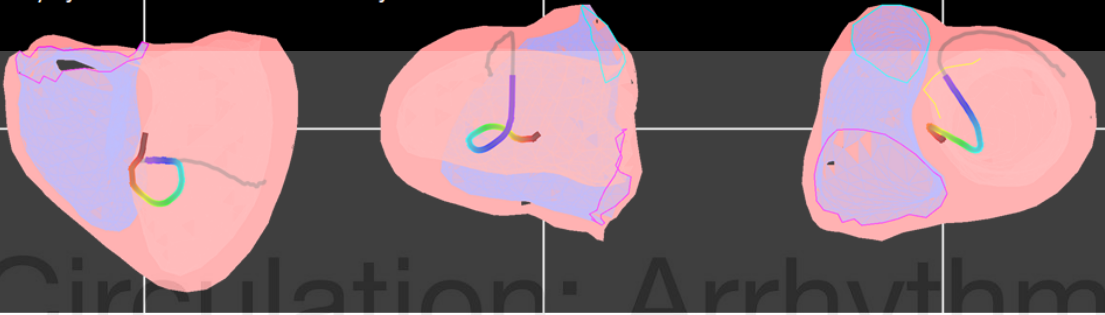
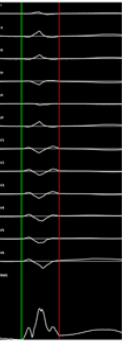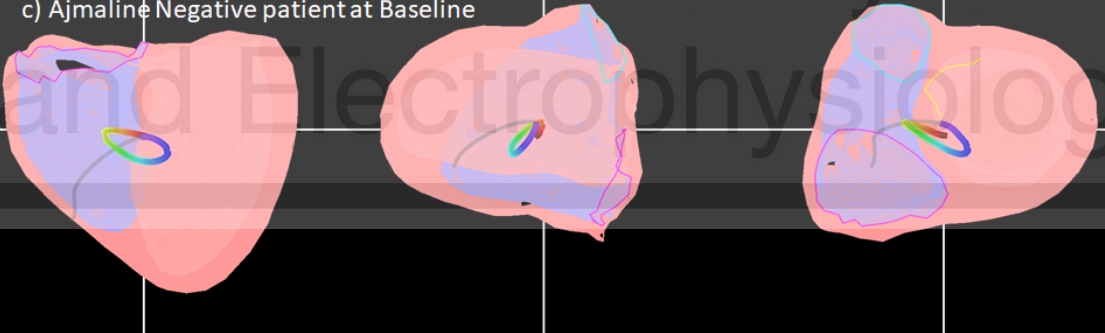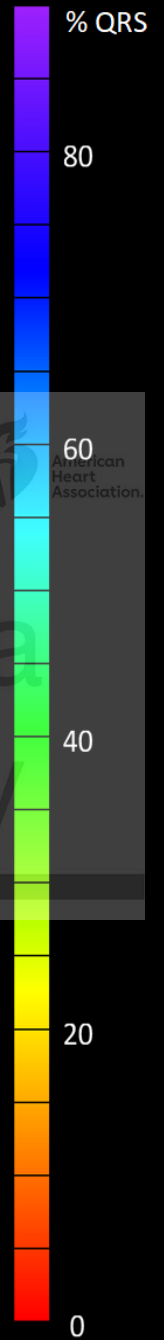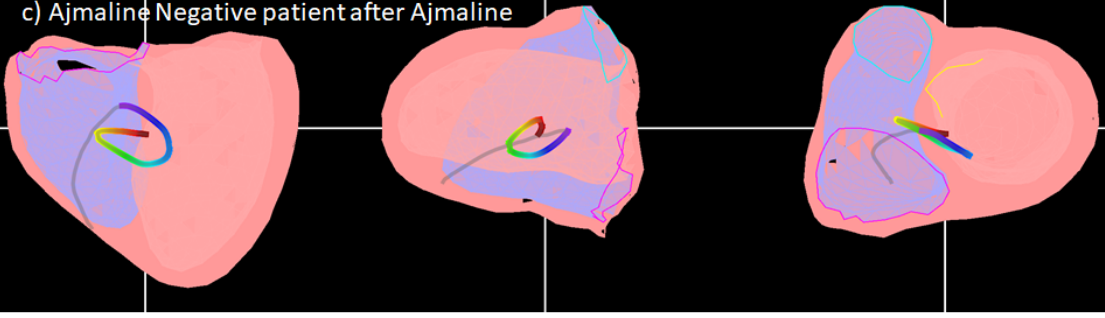b) Ajmaline-induced BrS

iECG indicated area
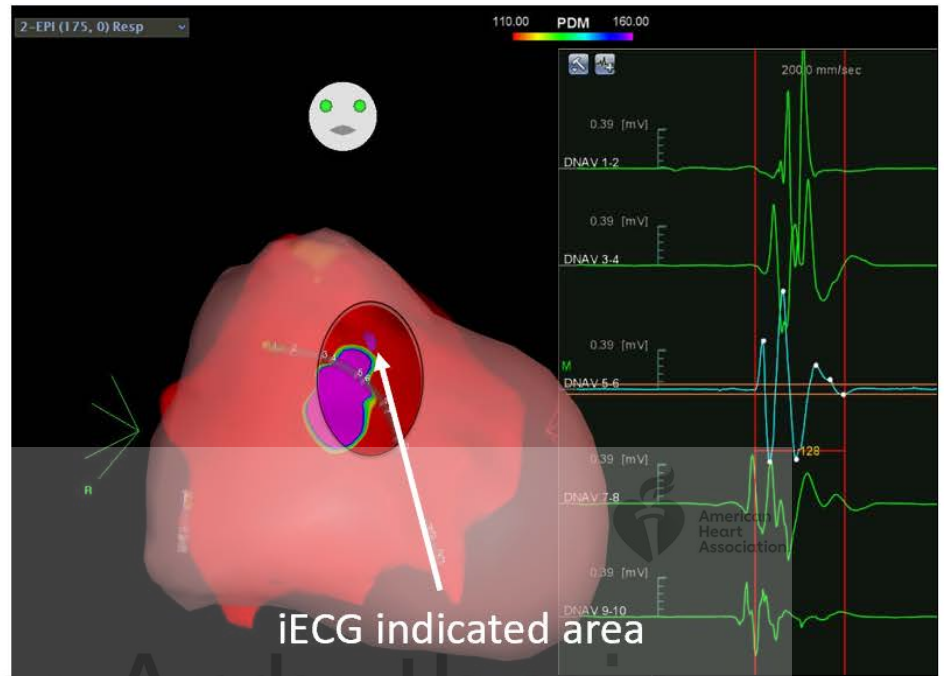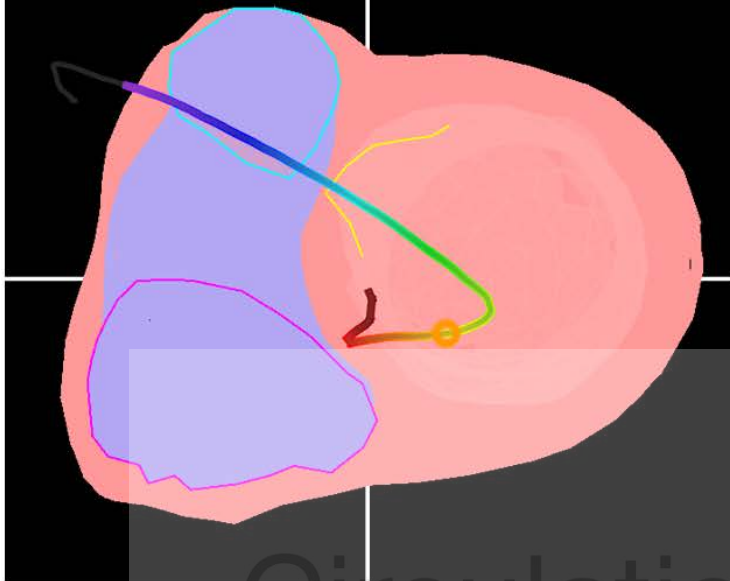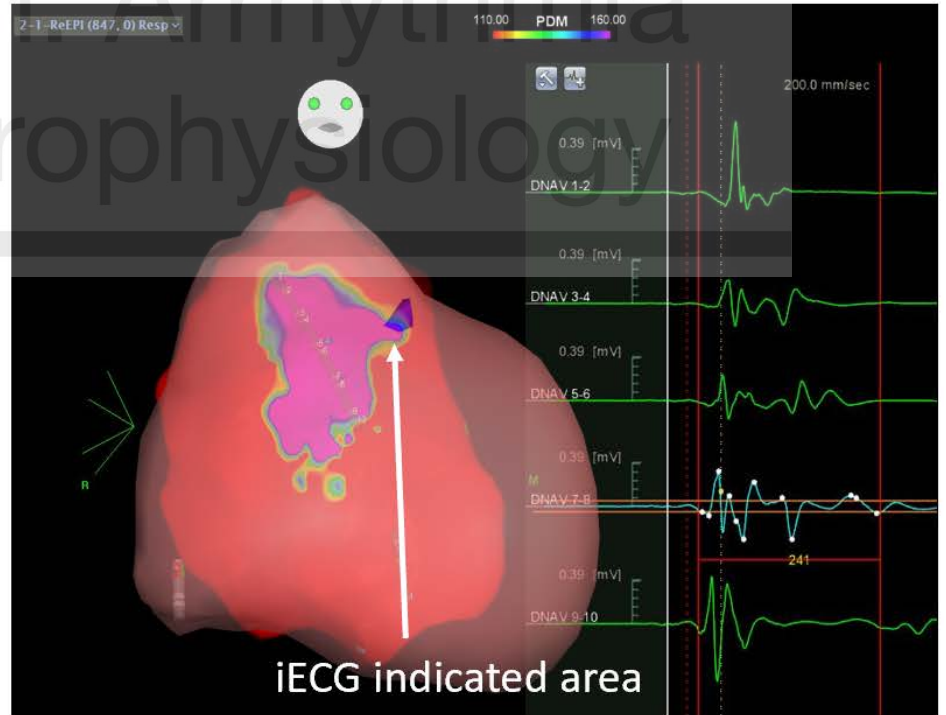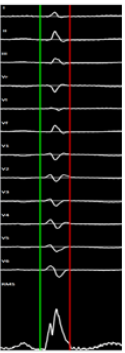
a) Ajmaline-induced BrS at Baseline

b) Ajmaline-induced BrS after Ajmaline

c) Ajmaline Negative patient at Baseline

c) Ajmaline Negative patient after Ajmaline

% QRS

80

60

40

20

0

CineECG: The link between ECG and cardiac anatomy
Localization of the Brugada Pattern to the RVOT